Published in final edited form as:
J Magn Reson. 2008 December ; 195(2): 219–225. doi:10.1016/j.jmr.2008.09.012.

Clinical NOE ^{13}C MRS for Neuropsychiatric Disorders of the Frontal Lobe

Napapon Sailasuta[a], **Larry W. Robertson**[b], **Kent C. Harris**[a], **Andrea L. Gropman**[c], **Peter S. Allen**[d], and **Brian D. Ross**[a]

[a]Huntington Medical Research Institutes, Pasadena,CA, USA

[B]Spin Dynamics, South Pasadean,CA, USA

[c]Department of Neurology, Children's National Medical Center, Washington D.C, USA

[d]Department of Biomedical Enginerring, Universit yof Alberta, AB, Canada.

1. Introduction

In vivo ^{13}C spectroscopy provides a unique way to study metabolic fluxes in human brain [1; 2;3]. Infusing highly enriched 13-carbon substrates such as glucose or acetate, together with complete proton decoupling which removes the proton splitting, results in carbon signal enhancement. These studies have been in the past invariably performed with WALTZ at 8 Watts or higher power proton decoupling schemes, on the posterior brain [4;5;6]. Important new information concerning control of the neuronal glial glutamate glutamine cycle has been derived from such studies. However, most higher executive functions are performed in frontal brain and many neuropsychiatric disorders including schizophrenia, HIV, drug abuse and depression are characterized by cognitive deficits involving the frontal lobes. Existing schemes for decoupling protons of C2, C3 and C4 ^{13}C resonances of Glu and Gln are prohibited in frontal structures, because of their potential to cause ocular damage. The lens of the human eye has reduced capacities to dissipate heat, due to its poor vascularization [7]. In an animal model, acute exposure of the eye to high power radiofrequency radiation has been shown to be cataractogenic [8]. In order to perform ^{13}C MRS studies safely in the human frontal lobe, therefore, a technique which involves very low or no RF-power deposition is necessary. By combining two well known features of ^{13}C NMR, we have been able to overcome these obstacles and have developed a means of safely monitoring ^{13}C fluxes of crucial metabolic pathways in frontal lobe structures in human volunteers and patients.

Specific enrichment and ready identification based upon differences in chemical shift of individual carbon atoms is one of the defining features of ^{13}C MRS [9;10] which makes it more informative than PET scanning.

Glutamate occurs in human brain at concentrations as high as 10mM and has been the subject of intensive research since discovery of the glial - neuronal glutamine-glutamate cycle in the

Correspondence to: Napapon Sailasuta.

1960's [11]. Glutamate has therefore been the most frequently studied amino acid in human ^{13}C neurospectroscopy studies.

Figure 1 illustrates the proton couplings of the five carbon neurotransmitter amino acid, glutamate. Carbons 2, 3 and 4 have one-bond proton coupling from proton directly attached where Carbon 1 and 5 have no directly attached proton. The carbonyl carbon (C5) is subject to dipolar interaction with surrounding water protons, a property employed in the present application to human brain since it renders C5 glutamate signal subject to enhancement via the low-power nuclear Overhauser effect (NOE). Commonly applied human and clinical ^{13}C protocols employ [1-13C] glucose (or [2-13C] acetate). By replacing as these precursors, both of which ^{13}C substrates initially enrich cerebral metabolic pools in coupled ^{13}C atoms, with ^{13}C substrates which enriches ^{13}C atoms not directly coupled to protons, ^{13}C label can be observed in a low power regime. ^{13}C signal enhancements occur in C5 Glu, C5 Gln and in the final oxidation products CO_2 and bicarbonate. The precursors [2-13C] glucose and acetate provide these results, in contrast to the more commonly employed substrates [1-13C] glucose and [2-13C] acetate, which do not.

To reduce the power deposition required for proton decoupling we propose to replace the high power WALTZ decoupling sequence by one which employs much lower power noise decoupling, together with nuclear Overhauser effect applied during acquisition. The nuclear Overhauser effect (NOE) is a cross-relaxation phenomenon commonly used in protein structural determination [12;13]. It involves two magnetically active nuclei in close proximity; saturating one nucleus for example, the proton will lead to an observable enhancement in the signal of the nuclei in close proximity, for example, the carbon resonances. Signal enhancement via the NOE mechanism can be realized using a low proton pulse power. NOE together with a proton decoupling have been shown to significantly enhance the signal-to-noise ratio and resolution in *in vivo* ^{31}P and ^{13}C MRS with typically lower proton NOE pulse power [14;15]. In this communication, we demonstrate the efficacy of this combined approach on phantoms and on the human brain in vivo. We confirm the potential for clinical application by *in vivo* acquisition of serial ^{13}C spectra from the frontal lobe of human subjects. (A preliminary account of these findings was presented as an Abstract at ISMRM, Toronto, 2008).

2. Results

Power Deposition

The local specific absorption rate (SAR) with the low power NOE pulse sequence was 0.8 +/− 0.1 (N=10)W/kg for the effected relevant portion of the posterior brain and < 0.8/0.6 = 1.25 Watts/kg for frontal brain which is well below the FDA guideline of 3 Watts/kg averaged over the head for 10 minutes [16;17;18]. Note that the higher SAR values from simulations by Wang et al [19] were based upon a whole head coil and do not apply to our data acquisition protocol.

Phantom studies

1). Noise schemes—Figure 2 shows the decoupling efficiency of different low power noise NOE schemes using dioxane. The proton frequency was set 100 Hz off resonance from water (4.7 ppm) for all experiments. It can been seen in figure 2B that using low power noise with a Gaussian filter gives comparable decoupling efficiency to that obtained with a high power WALTZ-4 NOE and decoupling scheme, and was superior to low power noise with sinc filter or that without any filter.

2). RF-power—Using the preferred NOE scheme, low power noise with a Gaussian filter, determined from figure 2, different decoupling power levels were evaluated and shown in

figure 3. An application of 0.5 W of low power is sufficient to fully decouple the dioxane resonance at 67 ppm, with negligible residual side bands.

3). Decoupling vs. NOE—We next compared the combined effects of low power noise decoupling and NOE on glutamate. Figure 4 illustrates the signal-to-noise gain for the non-protonated carbons C5 and C1 of glutamate and bicarbonate resonances in an aqueous solution of 1M natural abundance glutamate and 1M sodium bicarbonate, pH = 7.2. Note that based upon the equal natural abundance of ^{13}C = 1.1%, the intensities of C5 and C1 glutamate are equivalent Despite the lack of directly attached proton, some signal gain was achieved through application of low power noise NOE alone (figure 4B), and through lower power noise decoupling alone (figure 4C). It can be seen that the increase in signal-to-noise ratio of C1 and C5 resonances of glutamate achieved by combining low power noise NOE and decoupling is significant and equal to those from high power WALTZ-4 (compare figure 4D with figure 4E). This demonstration confirms the prediction, outlined in the introduction. Since there are only dipolar interaction and no proton-carbon scalar couplings to benefit from conventional proton decoupling, NOE is sufficient to achieve the required signal enhancement in both C1 and C5 glutamate and bicarbonate.

Human studies

Because many human brain spectra will necessarily include signal from scalp lipids, and because the critical C3, C4 of glutamate and glutamine co-resonate with these lipids, we first tested the low power noise decoupling and NOE sequence on the abundant and anatomically superficial lipids of the skull and scalp which require no ^{13}C enrichment for detection in only a few scans. Figure 5 compares natural abundance non-localized 13C spectra from the posterior region of head and brain of a healthy volunteer. With WALTZ-4 decoupling using proton decoupling power of 8W over a bandwidth of 1000Hz (B), the strongly coupled methylene, CH=CH resonances observed in the non-decoupled lipid spectrum (A) appear as singlets with higher signal intensity. When low power noise decoupling with Gaussian filter and proton decoupling power of 0.9W, and bandwidth 250 Hz was applied, the spectrum showed comparable decoupling efficiency in the glycerol and lipid –CH=CH- regions (C), results which confirm the effectiveness of NOE low power decoupling in vivo. Indeed the carbonyl resonance at 172 ppm in the low power NOE spectrum significant exceeded that obtained with WALTZ. Note however, that using the low power noise scheme substantial residual scalar proton coupling is still apparent in the methylene (–CH2) region. This is most probably the result of a much narrower bandwidth of 250Hz employed for noise decoupling compared to that applied with WALTZ-4 (1000Hz in this study). However, while this residual coupling in the 13C spectrum between 10 – 40 ppm can obscure C3, C4 of glutamate and glutamine; they are of little consequence for observation of the glutamate and glutamine C5 and bicarbonate resonances which occur in the well-decoupled spectral region above 100 ppm.

To directly observe cerebral C5 glutamate and C5 glutamine and bicarbonate in vivo in an acceptable acquisition time, human subjects received i–v infusions of 99% 13C enriched 1-13C glucose or 1-13C acetate. We have previously shown 1-13C glucose to enrich all five carbons of glutamate and glutamine as well as some metabolites of the TCA cycle, bicarbonate, and other amino acids in the human brain [20]. Using the standard high power proton decoupling scheme, enrichment of the C2, C3 and C4 pools of glutamate with ^{13}C was confirmed (results not shown). The efficacy of the proton low power noise scheme is demonstrated in figure 6. A 20 minute carbon MRS spectrum acquired during WALTZ-4 decoupling (figure 6A) and a spectrum acquired during low power noise decoupling and NOE (figure 6B), from the posterior parietal brain region of the subject during the same [1-13C] glucose infusion protocol, showed comparable signal to noise for the enriched ^{13}C brain C5 carbons of glutamate and glutamine and for ^{13}C bicarbonate. Thus, despite the fact that ^{13}C glucose enriches C5 glutamate,

glutamine and bicarbonate only after three turns of TCA cycle [21], using low power proton NOE yielded a signal-to-noise sufficient to provide diagnostic metabolic information from the posterior brain.

Representative spectra of the non-protonated carbon atoms of glutamate and bicarbonate were acquired from the parietal region of a patient. Twenty minute summed ^{13}C spectra with WALTZ-4 decoupling acquired 60 – 80 minutes after infusion commenced and twenty minute summed ^{13}C spectrum with low power NOE acquired in same subject, after 100 – 120 minutes are shown (Figure 6). Note that signal to noise were comparable, even though the spectra A and B were acquired 60 minutes apart, when fractional enrichment has begun to decline. The relatively weak enrichment in both spectra is accounted for by the use of precursor [1-13C] glucose which primarily enters the C2, 3 and 4 resonances of glutamate and glutamine, and only later enriches C5 (and C1) glutamate, glutamine and bicarbonate.

To reduce the duration of the experiment, optimize enrichment of the selected glutamate and glutamine carbon atoms and test the low power decoupling and NOE sequence for its performance in the frontal brain, we next examined a subject during and after infusion of [1-13C] acetate. We have previously shown this substrate to directly enrich C5 glutamate and glutamine during the first turn of the (glial) TCA cycle, and to release $^{13}CO_2$ immediately [22]. Using only the low power noise technique, C5 glutamine, C5 glutamate and ^{13}C bicarbonate were readily detected in 5 minutes. The brain structures examined are illustrated in the inset of figure8.

Consistent with the role of acetate as a fuel metabolized first in the cerebral glial compartment to glutamine, note the enrichment of $^{13}C5$ glutamine in the frontal cortex and the enrichment of $^{13}C5$ glutamate [22]. ^{13}C bicarbonate also appears in the frontal brain early in the time course of metabolism of [1-13C] acetate.

3. Discussion and Conclusion

We demonstrate in this study that low power noise for NOE enhancement in carbon MRS examinations renders carbon sites in the C5 of glutamate, glutamine and bicarbonate region visible. Sufficient signal-to-noise was achieved when labeled with enriched substrates at 1.5T to enable a number of critical tests of the new method. Notwithstanding the absence of directly attached protons, the $^{13}C5$ resonance can still benefit from proton excitation through NOE enhancement. Because the power deposited is within FDA guidelines for SAR in optic lens (4), this technique can now be routinely applied to the frontal lobe in common neuropsychiatric disorders, such as schizophrenia, HIV and those resulting from drug abuse, that are known to impact higher executive functions of the frontal lobe. It is expected to be a safe alternative to PET scanning, the only metabolic imaging technique currently applicable to all brain regions, including the frontal cortex and a complement to dynamic functional MRI studies, from which the metabolic substrate of brain activation is entirely lacking. Furthermore, because of radioactivity concerns, and because PET has only a limited role in the study of metabolic fluxes, the specific metabolic information contained in ^{13}C brain spectra promises an elegant technique to study brain metabolism in the frontal structures of the normal brain. Work is in progress in this Laboratory to explore abnormalities in cerebral glutamate metabolism hypothesized to be associated in many human neuropsychiatric and genetic conditions which primarily impact higher executive functions and other processes predominantly localized to frontal cortex. The precise neuropsychological functions which might thereby become accessible are determined to a large extent by the volume of interest (field of view; FOV) of the carbon 13 coil employed. The present prototype coil covers Brodmann areas 9 – 11, 46 and possibly 47, anatomically included in the dorsolateral prefrontal cortex, anterior prefrontal cortex, orbitofrontal area and inferior prefrontal gyrus. Now that feasibility has been established, it should be relatively

straightforward to design superior dual tuned RF coils which will increase available 13C SNR. Alternative strategies for amplifying ^{13}C signal in vivo include inverse detection and direct detection of labeled metabolites via proton MR spectroscopy [23] have been reported. We are optimistic that the new method of low power noise NOE will be applicable at 3 Tesla without exceeding SAR. Proton decoupling with WALTZ however, scales four-fold higher with increasing magnetic field and will therefore continue to present problems for human use in the frontal lobe. We are currently undertaking tests at 1.5, 3 and 4.7 Tesla to determine directly the RF power deposition and tissue temperature for each of the protocols introduced in this paper and will report the results separately.

Using dynamic nuclear polarization [24], PASADENA [25], xenon-13C transfer [26] or Brute-force techniques collectively termed high-definition MRI (HD-MRI) currently being explored in several Laboratories, may avoid the problems of SAR since proton decoupling is not employed with these methods. To date none of these methods has shown even pre-clinical results in the brain beyond angiography and the path to clinical utility and ^{13}C neurochemistry remains problematical. Nevertheless, if successful, HD-MRI with carbon 13 (and nitrogen 15) which will be performed without added RF-power deposition and by providing enormous signal gain (10,000 – 100,000 fold according to recent accounts) will encourage in vivo ^{13}C neurospectroscopy studies on the time scale and anatomic scale of milliseconds and millimeters, in contrast to the present report which achieves 5 – 20 minute time resolution over 10's of cubic centimeters of brain.

For the time being, however we believe that the present technique of low power direct detection of ^{13}C enriched glutamate, glutamine and bicarbonate, offers the best means of exploring human frontal brain disorders of glutamate neurotransmission and oxidative metabolism. Furthermore, since signal enhancement is due to long-range coupling to exchangeable water, it is highly likely to depend on brain physiology and might thereby, itself provide physiological information.

4. Methods

All proton decoupled ^{13}C MRS experiments were performed with approval of the Institutional Review Board (IRB) of Huntington Memorial Hospital and the Food and Drug Administration (FDA) Investigational New Drug (IND) 56510 ([1-13C] glucose) and IND 59950 ([1-13C] acetate) on a 1.5T Signa scanner equipped with broad-band exciter, a dual tuned half head (surface) 1H - 13C radiofrequency coil, a stand alone proton decoupler and a vector signal generator (Agilent E4433B). The RF head coil which could readily be dismounted from the MR scanner was applied either to the posterior parietal (occipital) region of the head or to the forehead, where the anterior portions of the frontal lobe were included in the field of view (see Insets to figure 6 and figure 7 for details of brain regions examined in the present study).

The RF-pulse sequences to be investigated included a variety of proton decoupling and NOE schemes and are illustrated in figure 8, where NOE (LPND) (figure 8D) refers to uninterrupted irradiation of low-power RF throughout the recovery time and the data acquisition window, and NOE+DC (figure 8E) refers to irradiation of low power RF during the recovery period and irradiation of high power RF during the acquisition window.

Random noise amplitudes and phases were created in Excel with three different filter schemes; Scheme1: normal random numbers with mean of 10 and standard deviation (SD) of 25 with pass-through filter, Scheme2: normal random numbers with mean of 10 and standard deviation (SD) of 25 with Sinc filter, and Scheme 3: pseudo random noise generation using the Box-Muller method [27] with mean of zero and SD of one with Gaussian filter. These schemes were downloaded onto the vector signal generator and executed at 8 KHz repetition rate. The

effective bandwidths of these random noise schemes were chosen at 250Hz, for comparison with the high power WALTZ-4 scheme of the 1000 Hz bandwidth. A conventional rectangular 90-degree radio-frequency pulse and acquire data acquisition scheme was used with pulse width of 252 μsec (figure 8A). Spectra were recorded using a spectral width of 5000 Hz, 1024 data points and TR of 1.5sec. Proton pulse power for decoupling and NOE were the actual power measured in Watts (calibrated for cable loss), using an external power meter (Agilent E4418B), at the point prior to the RF coil transmit port and continuously displayed during phantoms and in vivo human studies. A 100% solution of dioxane was used to characterize the efficiency of proton decoupling in a coupled model system. A second phantom comprising 1M glutamate and 1M sodium bicarbonate was used to test sequences on coupled proton-carbon resonances relevant to human brain studies. To evaluate the efficacy of the low power noise decoupling and NOE (LPND, figure 8D) in vivo, we compared the ^{13}C MRS spectra from the parietal brain region using WALTZ-4 decoupling with those acquired by low power noise NOE during an established ^{13}C substrate infusion protocol [2] , performed at a later time point during the same [1-13C] glucose infusion. In a second experiment, the RF- head coil was repositioned over the forehead of a different volunteer and a complete [1-13C]-acetate infusion using a low dose of 0.15g/kg body weight (3.3% w/v) of 99% enriched [1-13C]-acetate protocol was performed. ^{13}C MRS was performed with 13C low power proton noise NOE (LPND) acquisition from the frontal lobe. The [1-13C] acetate from Cambridge Isotope Laboratories was prepared as a pyrogen free solution by Fairview Pharmacy, Minneapolis, Mn. (Ms. Darlette Luke) and infused through the antecubital vein over 60 minutes[22]. Written informed consent was obtained. Axial T1-weighted MR images were acquired and used as a guide for homogeneity adjustment prior to ^{13}C MRS acquisition using a simple pulse-acquire data acquisition sequence (LPND, figure8D), together with low power pulses of 0.9 Watts. ^{13}C data acquisition commenced at the start of the infusion and was continued in five minute blocks for 120 minutes.

References

1. Rothman DL, Novotny EJ, Shulman GI, Howseman AM, Petroff OA, Mason G, Nixon T, Hanstock CC, Prichard JW, Shulman RG. 1H-[13C] NMR measurements of [4-13C]glutamate turnover in human brain. Proc Natl Acad Sci U S A 1992;89:9603–9606. [PubMed: 1409672]
2. Bluml S, Moreno-Torres A, Ross BD. [1-13C] glucose MRS in chronic hepatic encephalopathy in man. Magn Reson Med 2001;45:981–993. [PubMed: 11378875]
3. Shen J, Petersen KF, Behar KL, Brown P, Nixon TW, Mason GF, Petroff OA, Shulman GI, Shulman RG, Rothman DL. Determination of the rate of the glutamate/glutamine cycle in the human brain by in vivo 13C NMR. Proc Natl Acad Sci U S A 1999;96:8235–8240. [PubMed: 10393978]
4. Mason GF, Pan JW, Chu WJ, Newcomer BR, Zhang Y, Orr R, Hetherington HP. Measurement of the tricarboxylic acid cycle rate in human grey and white matter in vivo by 1H-[13C] magnetic resonance spectroscopy at 4.1T. J Cereb Blood Flow Metab 1999;19:1179–1188. [PubMed: 10566964]
5. Bluml S, Moreno A, Hwang JH, Ross BD. 1-(13)C glucose magnetic resonance spectroscopy of pediatric and adult brain disorders. NMR Biomed 2001;14:19–32. [PubMed: 11252037]
6. Kanamori K, Kondrat RW, Ross BD. 13C enrichment of extracellular neurotransmitter glutamate in rat brain--combined mass spectrometry and NMR studies of neurotransmitter turnover and uptake into glia in vivo. Cell Mol Biol (Noisy-le-grand) 2003;49:819–836. [PubMed: 14528919]
7. Shellock FG. Radiofrequency energy-induced heating during MR procedures: a review. J Magn Reson Imaging 2000;12:30–36. [PubMed: 10931562]
8. Shellock FG. Thermal responses in human subjects exposed to magnetic resonance imaging. Ann N Y Acad Sci 1992;649:260–272. [PubMed: 1580498]
9. Sherry AD, Zhao P, Wiethoff A, Malloy CR. 13C isotopomer analyses in intact tissue using [13C] homonuclear decoupling. Magn Reson Med 1994;31:374–379. [PubMed: 8208112]
10. Malloy CR, Sherry AD, Jeffrey FM. Analysis of tricarboxylic acid cycle of the heart using 13C isotope isomers. Am J Physiol 1990;259:H987–H995. [PubMed: 1975735]

11. Berl S, Nicklas WJ, Clarke DD. Compartmentation of citric acid cycle metabolism in brain:labelling of glutamate, glutamine, aspartate and gaba by several radioactive tracer metabolites. J Neurochem 1970;17:1009–1015. [PubMed: 4913269]
12. Egan W, Shindo H, Cohen JS. Carbon-13 nuclear magnetic resonance studies of proteins. Annu Rev Biophys Bioeng 1977;6:383–417. [PubMed: 17352]
13. Neuhaus, D.; Williamson, M. The Nuclear Overhauser Effect in Structural and Conformational Analysis. New York: Wiley; 2000.
14. Bluml S, Seymour KJ, Ross BD. Developmental changes in choline- and ethanolamine-containing compounds measured with proton-decoupled (31)P MRS in in vivo human brain. Magn Reson Med 1999;42:643–654. [PubMed: 10502752]
15. Bluml S, Tan J, Harris K, Adatia N, Karme A, Sproull T, Ross B. Quantitative proton-decoupled 31P MRS of the schizophrenic brain in vivo. J Comput Assist Tomogr 1999;23:272–275. [PubMed: 10096336]
16. Gruetter R, Adriany G, Merkle H, Andersen PM. Broadband decoupled, 1H-localized 13C MRS of the human brain at 4 Tesla. Magn Reson Med 1996;36:659–664. [PubMed: 8916015]
17. Bluml S. In vivo quantitation of cerebral metabolite concentrations using natural abundance 13C MRS at 1.5 T. J Magn Reson 1999;136:219–225. [PubMed: 9986765]
18. Guidelines for evaluating electromagnetic exposure risk for trials of clinical NMR systems. US: Center for Devices and Radiological Health, Food and Drug Administration; 1982 Feb 25.
19. Wang Z, Lin JC, Mao W, Liu W, Smith MB, Collins CM. SAR and temperature: simulations and comparison to regulatory limits for MRI. J Magn Reson Imaging 2007;26:437–441. [PubMed: 17654736]
20. Sibson NR, Dhankhar A, Mason GF, Behar KL, Rothman DL, Shulman RG. In vivo 13C NMR measurements of cerebral glutamine synthesis as evidence for glutamate-glutamine cycling. Proc Natl Acad Sci U S A 1997;94:2699–2704. [PubMed: 9122259]
21. Cruz F, Cerdan S. Quantitative 13C NMR studies of metabolic compartmentation in the adult mammalian brain. NMR Biomed 1999;12:451–462. [PubMed: 10654292]
22. Bluml S, Moreno-Torres A, Shic F, Nguy CH, Ross BD. Tricarboxylic acid cycle of glia in the in vivo human brain. NMR Biomed 2002;15:1–5. [PubMed: 11840547]
23. Boumezbeur F, Besret L, Valette J, Vaufrey F, Henry PG, Slavov V, Giacomini E, Hantraye P, Bloch G, Lebon V. NMR measurement of brain oxidative metabolism in monkeys using 13C-labeled glucose without a 13C radiofrequency channel. Magn Reson Med 2004;52:33–40. [PubMed: 15236364]
24. Ardenkjaer-Larsen JH, Fridlund B, Gram A, Hansson G, Hansson L, Lerche MH, Servin R, Thaning M, Golman K. Increase in signal-to-noise ratio of > 10,000 times in liquid-state NMR. Proc Natl Acad Sci U S A 2003;100:10158–10163. [PubMed: 12930897]
25. Bhattacharya P, Harris K, Lin AP, Mansson M, Norton VA, Perman WH, Weitekamp DP, Ross BD. Ultra-fast three dimensional imaging of hyperpolarized 13C in vivo. Magma 2005;18:245–256. [PubMed: 16320090]
26. Lisitza, N.; Chekmenev, EY.; Muradian, I.; Frederick, E.; Patz, S.; Hatabu, H.; Weitekamp, D.; Ross, BD. Enhanced Biomedical 13C NMR by Thermal Mixing with Hyperpolarized 129Xe. San Diego: ICMRB; 2008.
27. Lee J. A hardware Gaussian noise generator using the Box-Muller method and its error analysis. Computers, IEEE transaction 2007;55:657–671.

Acknowledgments

Supported by NCRR K12RR17613, U54RR019453-04, 1M01RR020359, 010058 (AG), NIDAK2521112 (NS), NARSAD Mental Health Research Association (KH), Alberta Heritage Fund (PSA), NIH NS4589 (BDR) and Rudi Schulte Research Institute (BDR). We thank Cambridge Isotopes for providing a travel grant to one of us (PSA). The authors are grateful to Osama Abulseoud MD for assistance with I-V protocols.

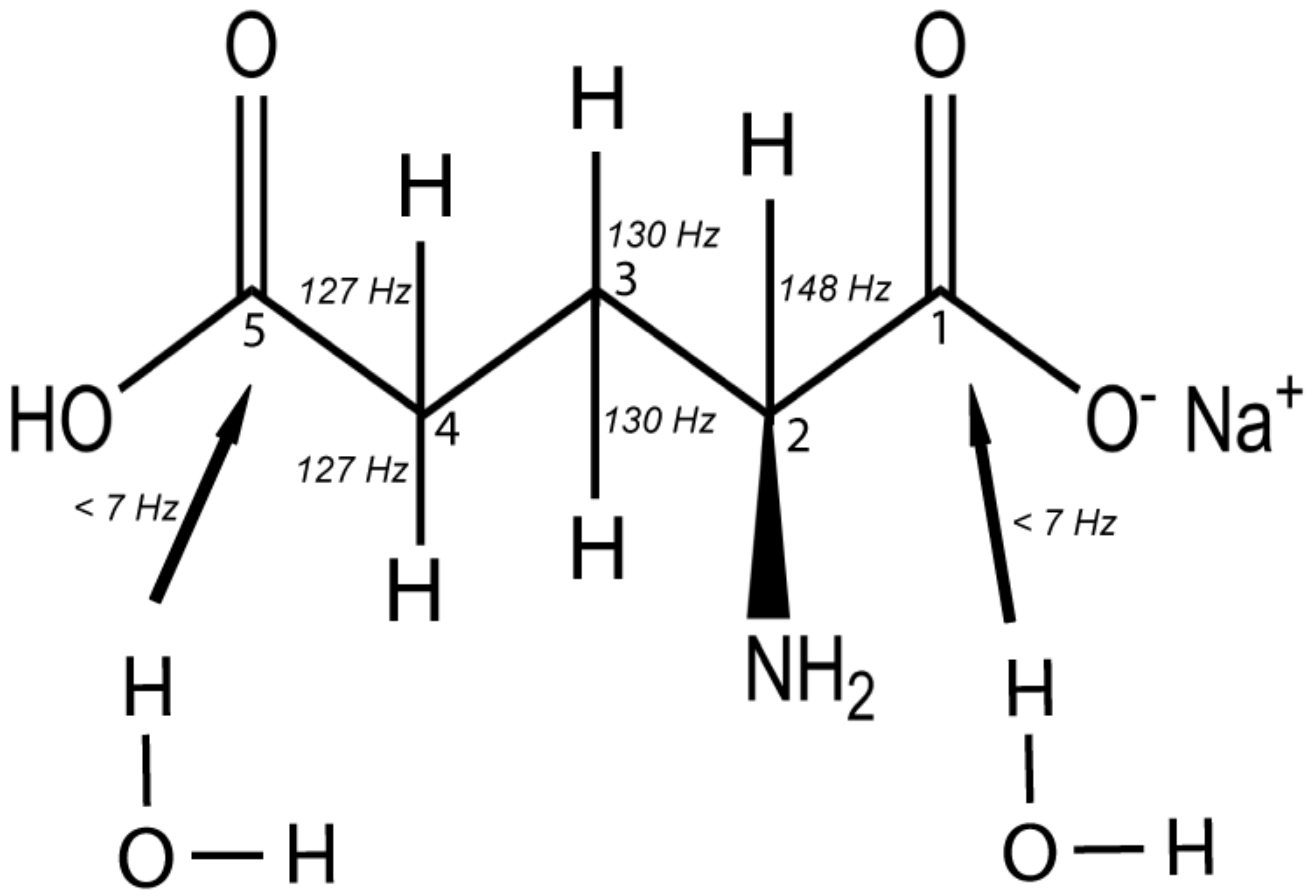

Figure 1.
Chemical structure of glutamate showing C2, C3 and C4 carbons with their scalar couplings (J-coupling constant indicated) to protons whereas C5 and C1 carbons are not directly coupled to protons but may interact via dipolar coupling with water molecule.

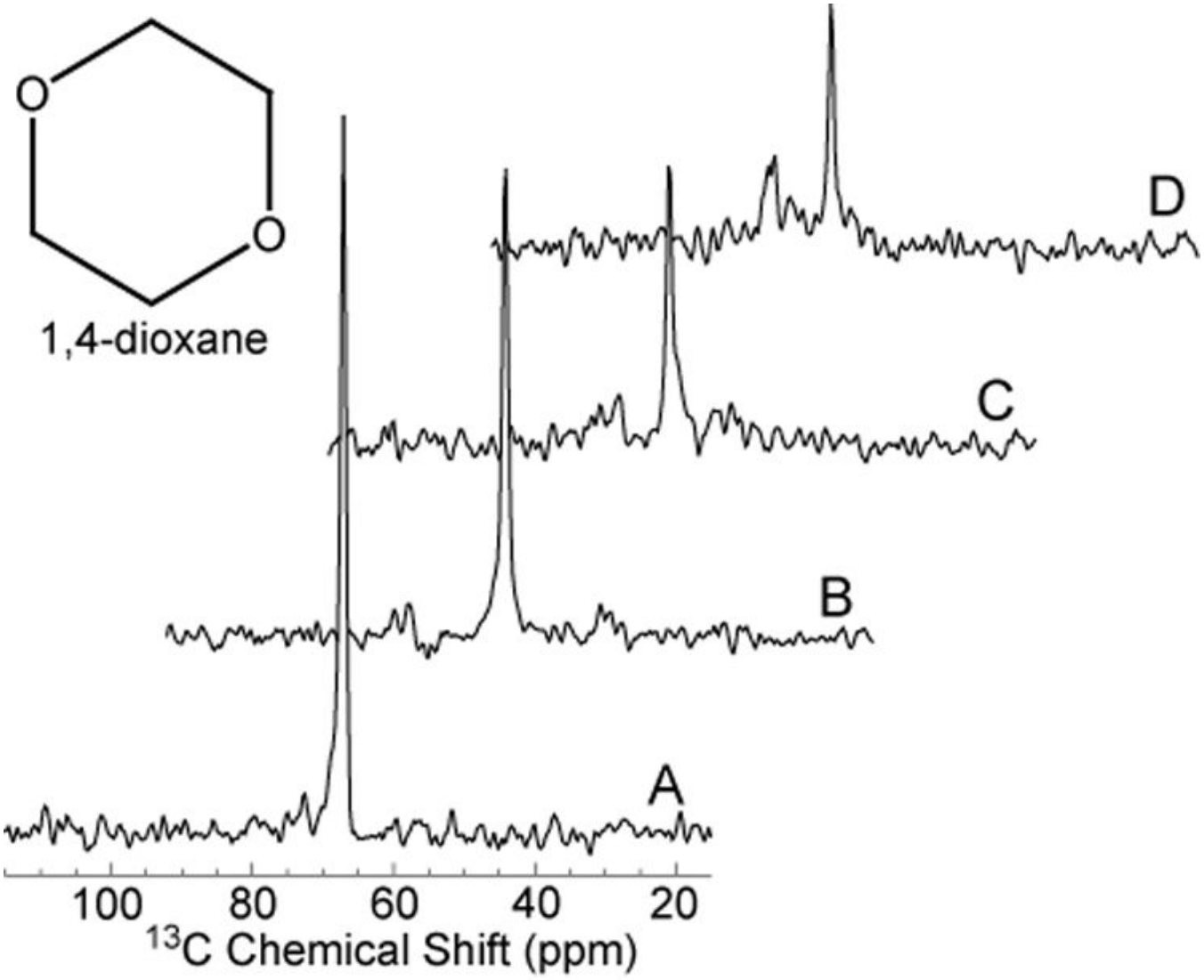

Figure 2.

Proton Decoupled ^{13}C spectra of dioxane. Experiments were performed in a 1.5 Tesla clinical MR scanner using dual tuned half-head coil previously described [2]. The various decoupling and NOE schemes described in Methods, (Figure 8), resulted in collapse of the coupled spins with incremental signal enhancement of the resulting 13C singlet resonance. The greatest signal enhancement was obtained with low power noise decoupling together with Gauss filter (Spectrum B). All spectra were scaled relative to the highest peak (Spectrum A).
A). High power WALTZ-4 NOE (0.6Watts) and decoupling (6 Watts), B). Low power noise NOE (0.5 Watts) and decoupling (0.5 Watts) with Gaussian filter C). Low power noise (0.5 Watts) and decoupling (0.5 Watts) with Sinc filter, D). Low power noise NOE (0.5 Watts) and decoupling (0.5 Watts) without filter.

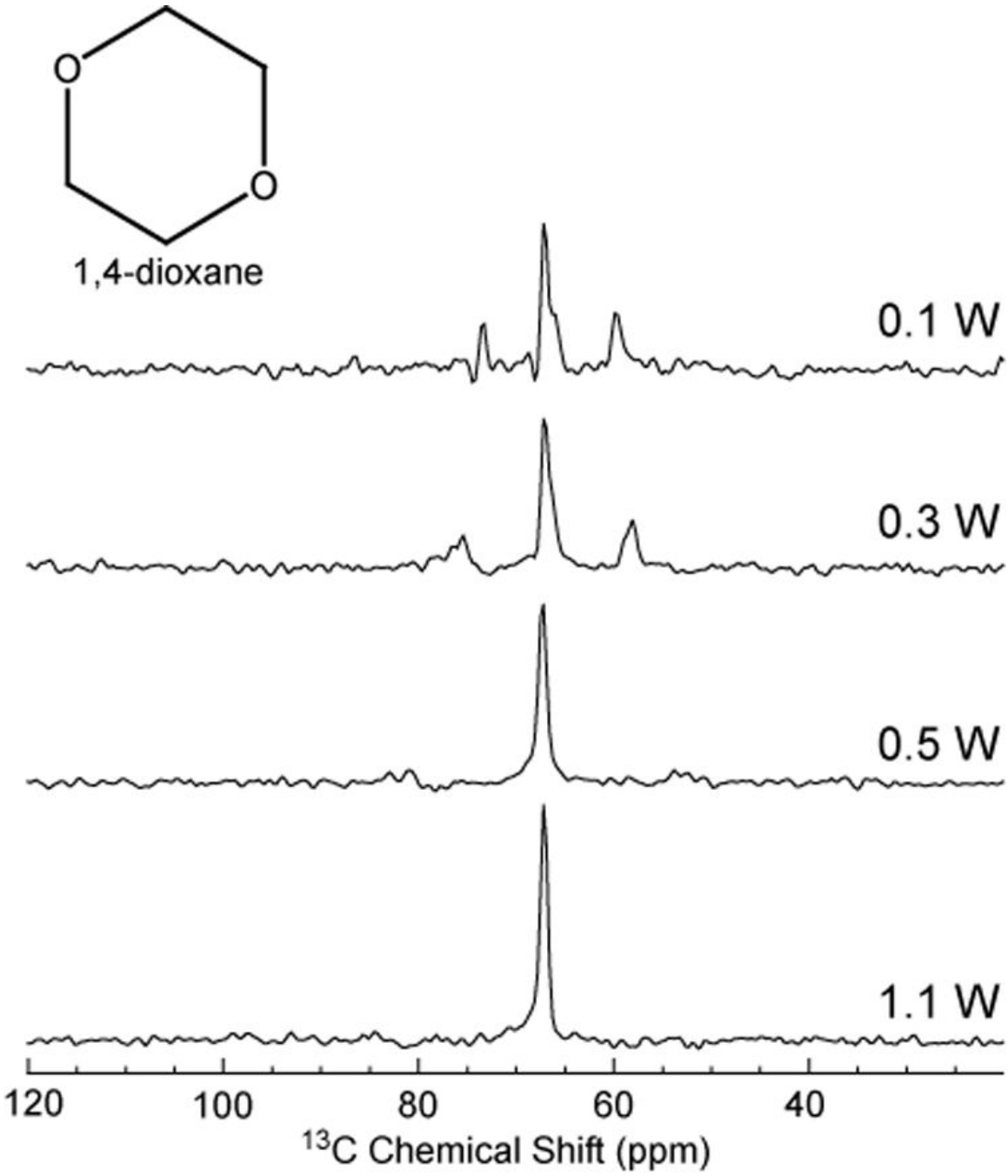

Figure 3.
Decoupling efficiency for 1,4 dioxane acquired using NOE and decoupling scheme in figure 8D at different decoupling powers.

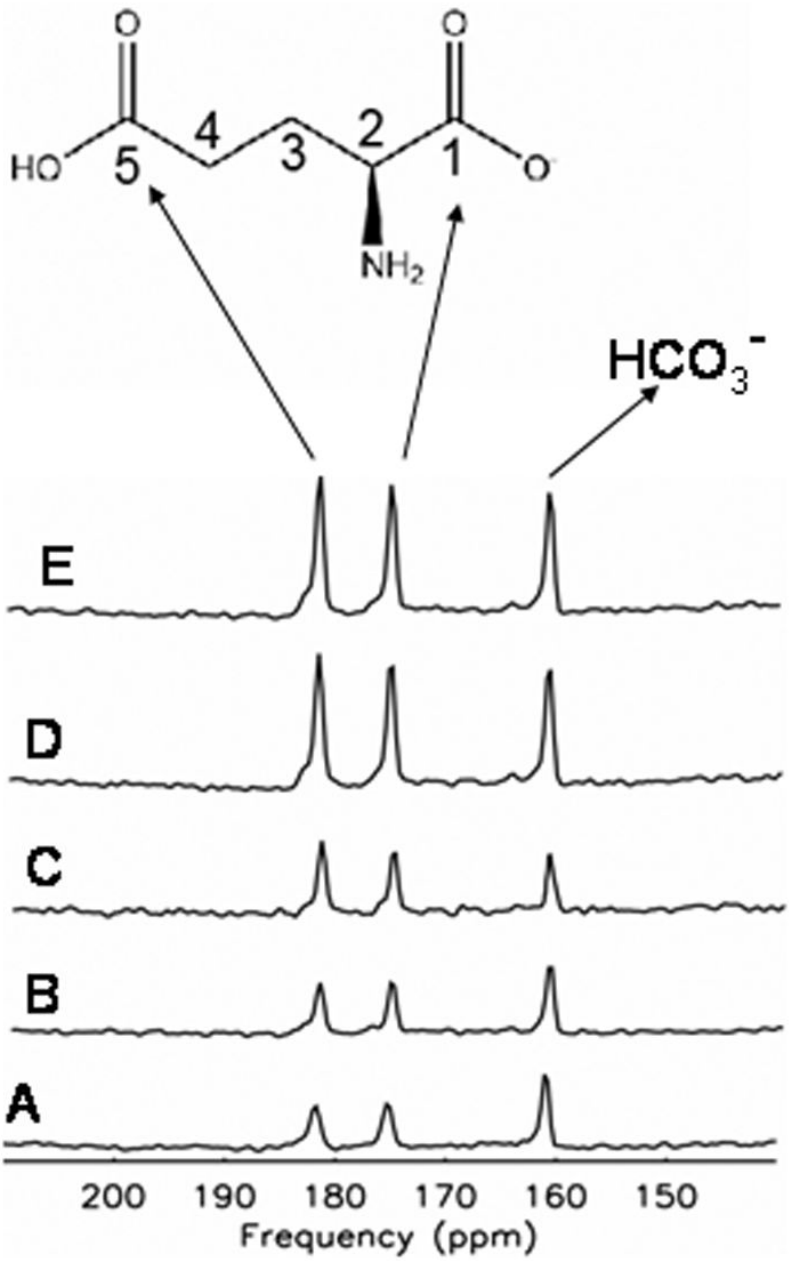

Figure 4.

Impact of NOE and decoupling on carbon atoms of glutamate and bicarbonate. Comparison of A). no decoupling or NOE (Figure 8A), B). low power noise decoupling alone (Figure 8C), C). low power noise NOE alone (Figure 8B), D). low power decoupling and NOE (LPND, Figure 8D), and E). high power WALTZ-4 decoupling and low power NOE (Figure 8E) of 1M glutamate and 1M Bicarbonate (HCO_3^-) indicates that in natural abundance glutamate, signal is almost equally enhanced by either high power proton decoupling or low power decoupling and NOE.

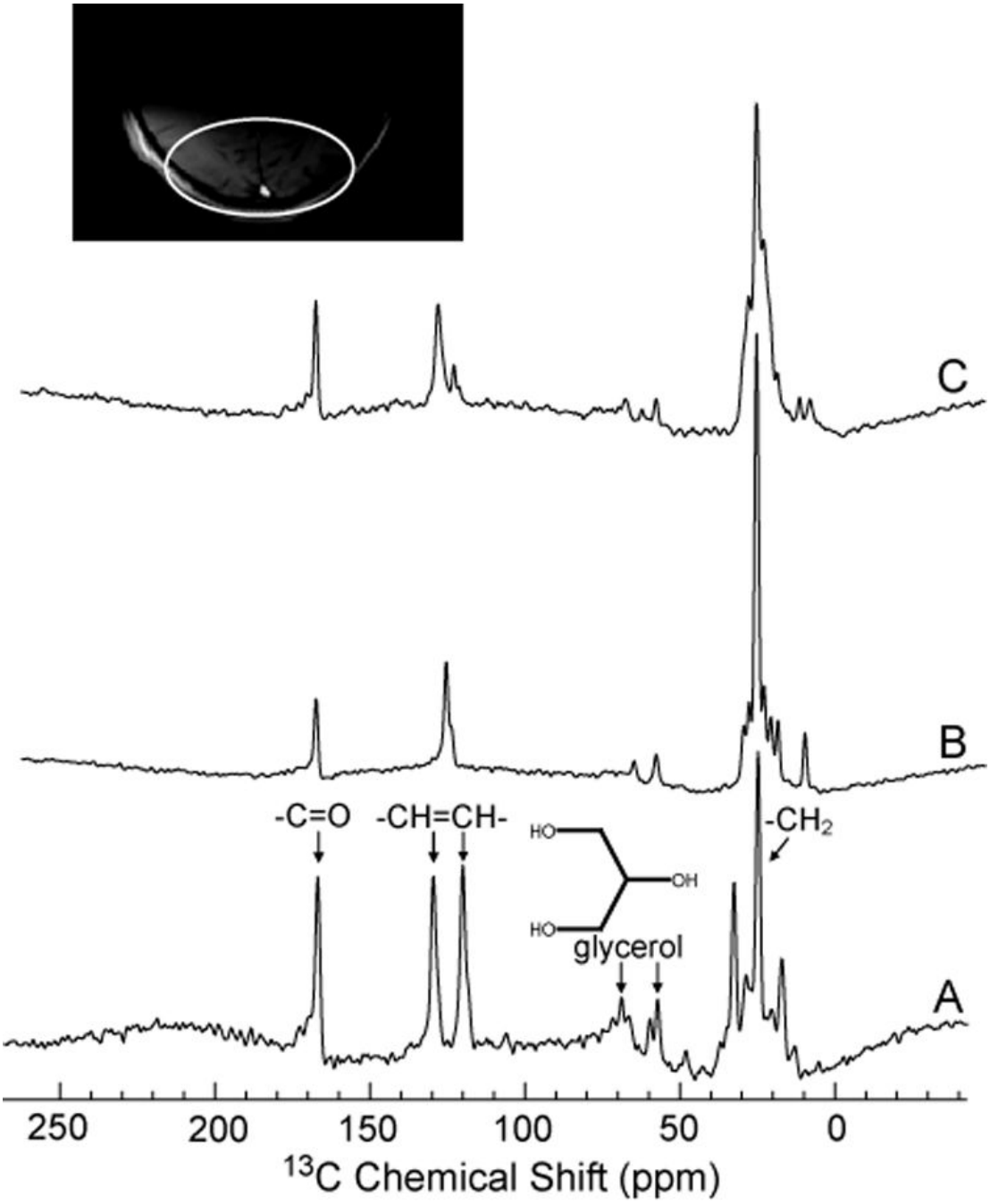

Figure 5.
Natural abundance 13C MRS lipid spectra from the human head in vivo. A): no decoupling or NOE, B): high power proton decoupling and NOE (WALTZ-4 at 8W, figure 8E), C): low power NOE (figure 8D) (0.9W). Proton frequency for both B) and C) was set to 100Hz from water (approximately 3 ppm). Note that Spectrums B and C are scaled to each other; peak intensities can be directly compared. Spectrum A has not been scaled and is provided as a chemical shift reference.

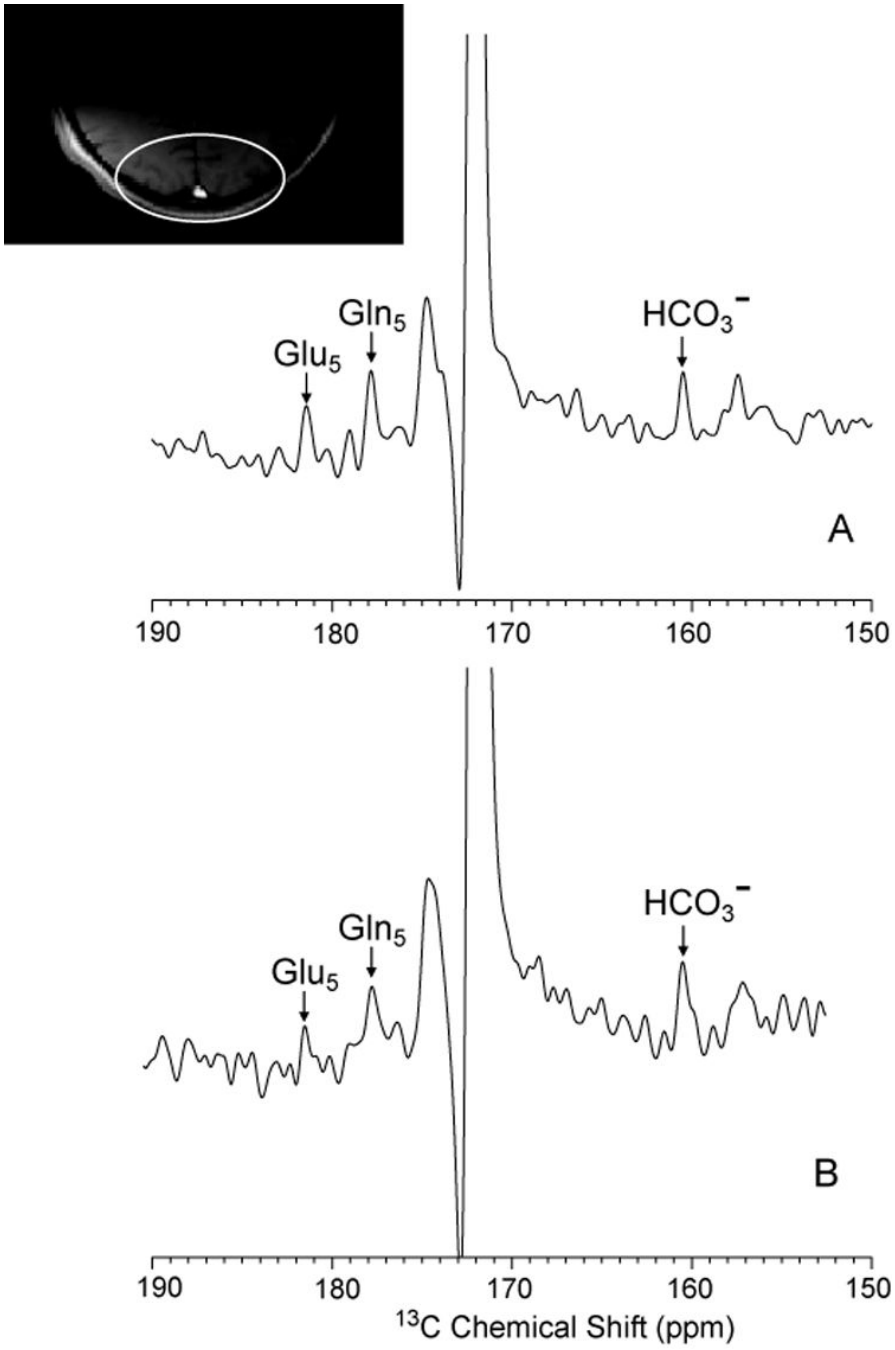

Figure 6.
Comparison of NOE + DC (Figure 8E scheme) (A) and low power NOE (LPND, figure 8D scheme) (B) of the posterior parietal human brain in an [1-13C] glucose infusion protocol. The enrichment of ^{13}C in glutamate, glutamine and bicarbonate region is shown.

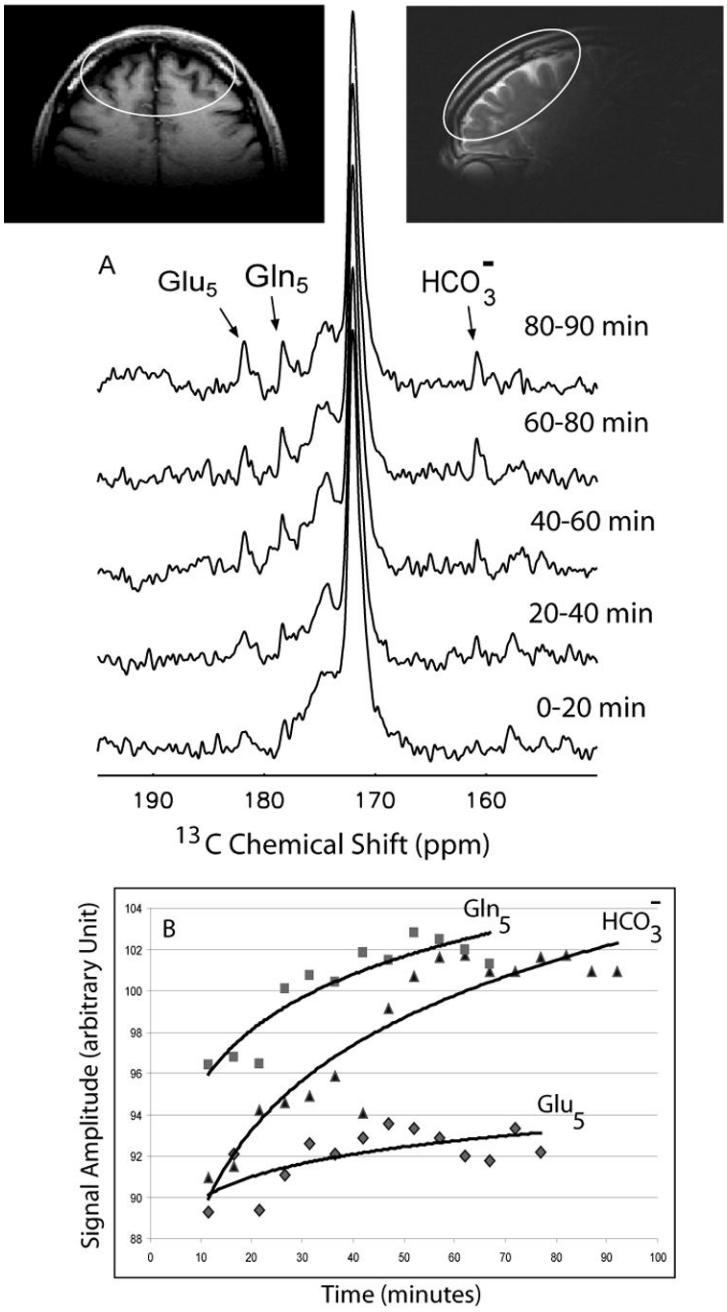

Figure 7.

Enrichment of 13C in glutamate and glutamine in the anterior (frontal) brain during 1-13C acetate infusion.

A). Sequentially acquired ^{13}C spectra are shown for 20 minutes increments from the start of the infusion, with the appearance of $^{13}C5$ glutamate and $^{13}C5$ glutamine and bicarbonate resonances (Figure 7A). B). The complete time course of accumulation of enriched metabolites over time are shown at 5 minute intervals. (Note: Signal amplitudes for Gln_5, Glu_5 and HCO_3^- are not to scale) Inserts are axial and sagittal images showing that Broadmann areas 9–11, 46 and possibly 47 of frontal cortex are included in the MRS field of view.

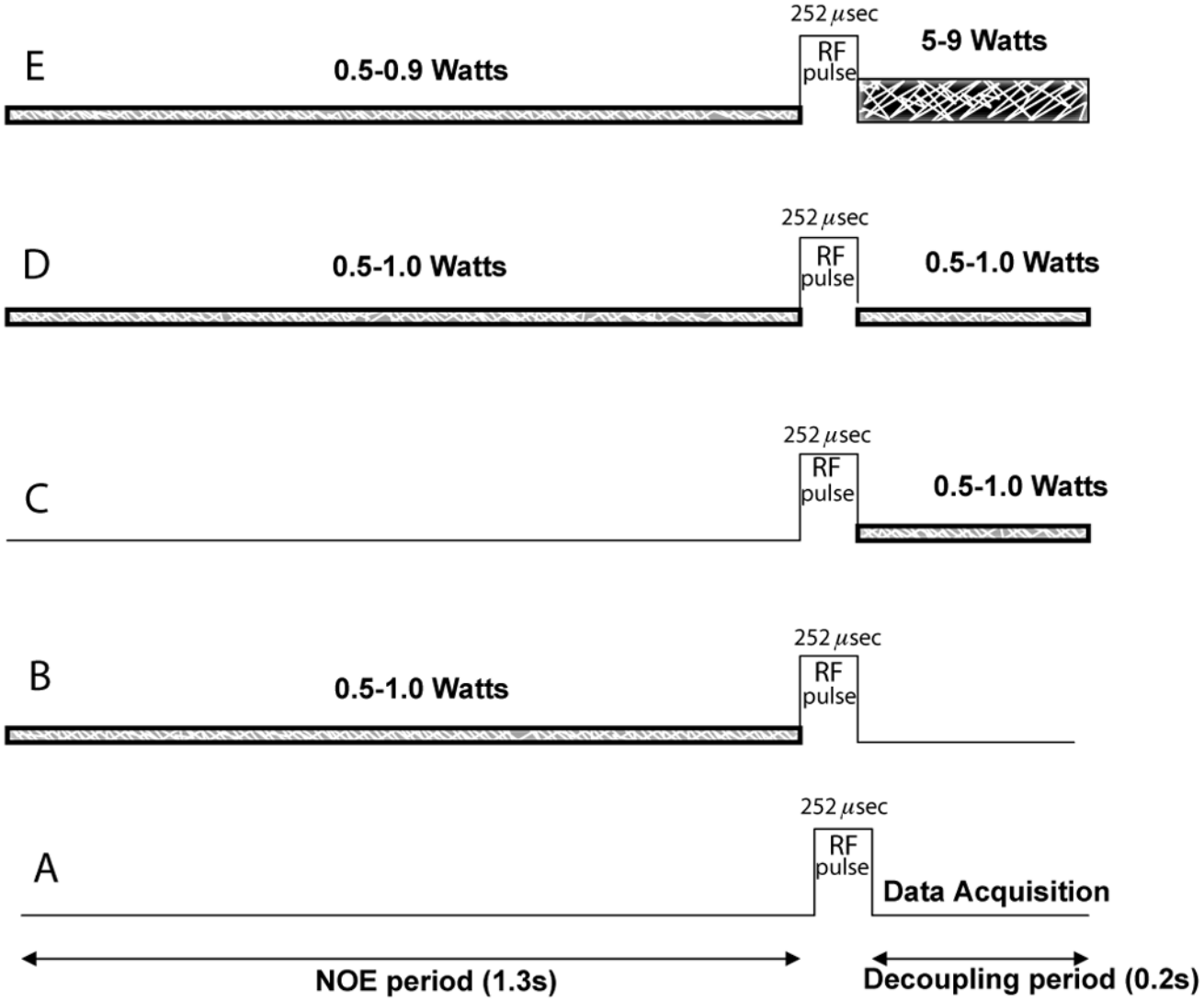

Figure 8.

Different proton decoupling and NOE schemes employed in this study. A). No decoupling and NOE, B). Low power noise (1.0-0.5 Watts) NOE only, C). Low power noise (1.0-0.4 Watts) decoupling only, D). Low power noise (1.0-0.5 Watts) for NOE and for decoupling (LPND), E). Low power WALTZ-4 NOE (0.9-0.5 Watts) and decoupling (5–9 Watts). Bandwidth of NOE applied was 250Hz and of Waltz-4, 1000Hz.